


# Resistance Evolution against Host-directed Antiviral Agents: Buffalopox Virus Switches to Use p38- $\gamma$ under Long-term Selective Pressure of an Inhibitor Targeting p38- $\alpha$

Yogesh Chander,<sup>†,1,2</sup> Ram Kumar,<sup>†,1</sup> Assim Verma,<sup>1,2</sup> Nitin Khandelwal,<sup>1</sup> Himanshu Nagori,<sup>1</sup> Namita Singh,<sup>2</sup> Shalini Sharma,<sup>3</sup> Yash Pal,<sup>1</sup> Apurvasinh Puvar,<sup>4</sup> Rameshchandra Pandit,<sup>4</sup> Nitin Shukla,<sup>4</sup> Priyank Chavada,<sup>4</sup> Bhupendra N. Tripathi,<sup>†,1</sup> Sanjay Barua,<sup>\*,1</sup> and Naveen Kumar <sup>\*,1</sup>

<sup>1</sup>National Centre for Veterinary Type Cultures, ICAR-National Research Centre on Equines, Hisar, India

<sup>2</sup>Department of Bio and Nano Technology, Guru Jambheshwar University of Science and Technology, Hisar, Haryana, India

<sup>3</sup>Department of Veterinary Physiology and Biochemistry, Lala Lajpat Rai University of Veterinary and Animal Sciences, Hiar, Haryana, India

<sup>4</sup>Gujarat Biotechnology Research Centre, Department of Science & Technology, Government of Gujarat, Gandhinagar, India

<sup>†</sup>These authors contributed equally to this work.

<sup>\*</sup>Present address: Animal Science Division, Indian Council of Agricultural Research, Krishi Bhawan, New Delhi

**\*Corresponding authors:** E-mails: sbarua06@gmail.com; naveenkumar.icar@gmail.com.

**Associate editor:** Xuhua Xia

## Abstract

Host-dependency factors have increasingly been targeted to minimize antiviral drug resistance. In this study, we have demonstrated that inhibition of p38 mitogen-activated protein kinase (a cellular protein) suppresses buffalopox virus (BPXV) protein synthesis by targeting p38-MNK1-eIF4E signaling pathway. In order to provide insights into the evolution of drug resistance, we selected resistant mutants by long-term sequential passages ( $P$ ;  $n = 60$ ) in the presence of p38 inhibitor (SB239063). The P60-SB239063 virus exhibited significant resistance to SB239063 as compared to the P60-Control virus. To provide mechanistic insights on the acquisition of resistance by BPXV-P60-SB239063, we generated p38- $\alpha$  and p38- $\gamma$  (isoforms of p38) knockout Vero cells by CRISPR/Cas9-mediated genome editing. It was demonstrated that unlike the wild type (WT) virus which is dependent on p38- $\alpha$  isoform, the resistant virus (BPXV-P60-SB239063) switches over to use p38- $\gamma$  so as to efficiently replicate in the target cells. This is a rare evidence wherein a virus was shown to bypass the dependency on a critical cellular factor under selective pressure of a drug.

**Key words:** p38, SB239063, virus, switch to use alternate cellular factor, drug resistance, host-directed antiviral agents.

## Introduction

Buffalopox virus (BPXV) is a close variant of the vaccinia virus, the type-species of the genus *Orthopoxvirus*. BPXV causes pock-like lesions, primarily in domestic buffaloes (*Bubalus bubalis*), but cattle and humans can also be infected and hence is considered a potential zoonotic threat (Roy and Chandramohan 2021). Buffalopox is primarily restricted to the Indian subcontinent, but the infection has also been reported in Egypt, Russia, and Italy (Singh et al. 2007; Marinaik et al. 2018; Yadav et al. 2020; Roy and Chandramohan 2021). Currently, there is no specific vaccine or antiviral drug available against BPXV infection.

Out of the over 200 different pathogenic human viruses known, FDA-approved antiviral drugs are currently available only against a few of them, mostly against human immunodeficiency virus 1 (HIV-1), hepatitis C virus (HCV), hepatitis B virus (HBV), herpes simplex virus 1 (HSV-1), cytomegalovirus (CMV), and severe acute respiratory

syndrome coronavirus 2 (SARS-CoV-2). However, a major problem with the existing antiviral drugs is the rapid development of drug resistance due to mutations at the drug-gable sites. This has been a commonly observed phenomenon with most of the antiviral drugs available for clinical use so far.

Viruses are highly dependent on the cellular machinery for replication. At the same time, host cells also encode several antiviral cellular proteins to block virus replication. This arms race influences virus replication, tropism, and disease severity (Dou et al. 2018; Kumar et al. 2018b; Long et al. 2019). The cellular proteins that interfere with the virus replication are antiviral factors, while those that support the virus perform pro-viral roles, are host dependency factors (HDFs) (Lv and Zhang 2021). These HDFs which participate in the battle between pathogen and host are often under strong evolutionary pressure. Despite the advent of powerful systems-level methodologies (omics approaches),

© The Author(s) 2022. Published by Oxford University Press on behalf of Society for Molecular Biology and Evolution.

This is an Open Access article distributed under the terms of the Creative Commons Attribution-NonCommercial License (<https://creativecommons.org/licenses/by-nc/4.0/>), which permits non-commercial re-use, distribution, and reproduction in any medium, provided the original work is properly cited. For commercial re-use, please contact [journals.permissions@oup.com](mailto:journals.permissions@oup.com)

Open Access

there is a significant gap in our understanding about the precise function of various HDFs in virus replication. Since viruses cannot easily regain the depleted cellular functions by mutagenesis, therefore it is believed that viruses are unlikely to generate resistant mutants against agents that target HDFs (Kumar et al. 2018b). Nevertheless, resistant virus variants against host-directed agents could still occur at a relatively low level upon long-term exposure to the host-directed agents (Hoffmann et al. 2011; Krumm et al. 2011; Kumar et al. 2011b, 2022). However, the mechanisms underlying acquisition of resistance by the viruses against host-directed agents is poorly understood.

By screening a library of small molecule chemical inhibitors, we identified p38 mitogen-activated protein kinase (p38 MAPK) inhibitor SB239063 as one of the potential hit that resulted in reduced BPXV replication *in vitro*. p38 is a serine/threonine protein kinases which transduces signals from inflammation stimuli. There are four genes encoding p38 MAPK family members in mammals, namely, p38- $\alpha$  (MAPK14), p38- $\beta$  (MAPK11), p38- $\gamma$  (MAPK12/extracellular signal-related kinase [ERK]-6), and p38- $\delta$  (MAPK13/SAPK4) with the p38- $\alpha$  isoform being the most abundant in the majority of cell types (Jiang et al. 1996, 1997; Enslin et al. 1998; Avitzour et al. 2007; Cuenda and Rousseau 2007; Rodriguez Limardo et al. 2011). These isoforms are co-expressed and may be co-activated in the same cell (Avitzour et al. 2007).

Based on sequence similarity, cellular expression patterns, and substrate specificity, p38 MAPK family is divided into two subgroups (Risco and Cuenda 2012). The first group consists of p38- $\alpha$  and p38- $\beta$  which have sequence identity of over 75% and are ubiquitously expressed in most cells types (Enslin et al. 1998). p38- $\gamma$  and p38- $\delta$  represent another subgroup with sequence identity of ~70% (Jiang et al. 1996, 1997; Rodriguez Limardo et al. 2011). p38- $\gamma$  and p38- $\delta$  have ~61% sequence identity to p38- $\alpha$ /p38- $\beta$  and are expressed only in certain cell types (Risco and Cuenda 2012).

Long-term sequential passage ( $n = 60$ ) of BPXV in the presence of SB239063 (inhibitor of p38- $\alpha$  and p38- $\beta$  but not p38- $\gamma$ ) (Cuenda et al. 1997; Kumar et al. 1997; Kuma et al. 2005; Cuenda and Rousseau 2007) resulted in the generation of mutant virus (P60-SB239063) which replicated more efficiently in p38- $\alpha$  KO as compared to p38- $\gamma$  KO cells. This is a rare evidence on bypassing the dependency of a critical cellular factor by a virus.

## Results

### p38 Inhibition Suppresses BPXV Replication

In order to evaluate the role of p38 in BPXV replication, we primarily employed SB239063 and SB203580, chemical inhibitors of p38- $\alpha$ /p38- $\beta$ . Their cytotoxic concentration 50 (CC<sub>50</sub>) in Vero cells, as determined by MTT [(3-(4,5-dimethylthiazol-2-yl)-2,5-diphenyltetrazolium bromide)] assay, were 57.6  $\mu$ g/mL and 16.2  $\mu$ g/mL respectively (Fig. 1A1 and A2). In order to determine the antiviral efficacy, we used sub-cytotoxic

concentrations ( $\leq 15$   $\mu$ g/mL and  $\leq 2$   $\mu$ g/mL respectively for SB239063 and SB203580) and measured the yields of infectious BPXV in Vero cells wherein a dose-dependent antiviral effect was observed (Fig. 1B1 and B2). To analyze the virucidal effects on extracellular virions, BPXV was incubated with various concentrations of the inhibitors for 90 min and then the residual infectivity was titrated on Vero cells. Infectious viral titers were comparable in both inhibitor- and dimethylsulfoxide (DMSO)-treated cells (Fig. 1C1 and C2), suggesting that both SB239063 and SB203580 do not exert any direct virucidal effect on BPXV and that their antiviral activity is presumably due to the inhibition of viral life cycle in the target cells.

### Generation of p38- $\alpha$ and p38- $\gamma$ knockout (KO) Cells

One of the possible mechanisms of acquisition of resistance against host-targeting agents is that the virus may switch to use alternate cellular factor/isoform (Hopcraft and Evans 2015; Kumar et al. 2020). Based on the amino acid sequence similarity, p38 is divided into two distinct subsets; the first group consists of p38- $\alpha$  and p38- $\beta$ , while the other p38- $\gamma$  and p38- $\delta$ . p38 inhibitors such as SB203580, SB202190 and SB239063 can inhibit p38- $\alpha$  and p38- $\beta$ , however p38- $\gamma$  and p38- $\delta$  remain completely unaffected (Cuenda et al. 1997; Kumar et al. 1997; Kuma et al. 2005; Cuenda and Rousseau 2007). In order to evaluate whether BPXV-P60-SB239063 has switched to use alternate host factor (p38- $\alpha$ /p38- $\beta$  to p38- $\gamma$ /p38- $\delta$ ), we first generated p38- $\alpha$  and p38- $\gamma$  KO cells by clustered regularly interspaced short palindromic repeats/CRISPR associated protein 9 (CRISPR/Cas9)-mediated genome editing wherein sgRNAs targeting the genes encoding p38- $\alpha$  and p38- $\gamma$  were cloned into pL.CRISPR.EFS.GFP and transfected to Vero cells. The GFP expressing cells were sorted by fluorescence activated cell sorter (FACS) and cultured in 96-well tissue culture plates by limiting dilution assay. After culturing for 1–2 weeks, the wells with a single clone ( $n = 11$ ) were selected (microscopy) for further propagation. To evaluate the gene editing, three to four clones were selected for polymerase chain reaction (PCR) amplification out of the 11 clones that were selected for propagation. As expected, wild type (WT) Vero cells resulted in an amplification of 441 nt long PCR fragment but the three p38- $\alpha$  KO clones ( $\alpha 3$ ,  $\alpha 6$ , and  $\alpha 10$ ) that were selected for evaluation had shortened length (260–328 nucleotides) of PCR products (Fig. 2A). This deletion was further confirmed by nucleotide sequencing (data not shown, sequences will be available on request). Finally, the clone 3 ( $\alpha 3$ ) which had a deletion of 113 nucleotides (nt 496–608) (Fig. 2B) and replicated slightly slower during initial passages was selected for further work. After four to five passages, the doubling times of  $\alpha 3$  clones were comparable with WT Vero cells (data not shown).

Four p38- $\gamma$  clones that were selected for propagation had similar length of PCR products as was observed in WT Vero cells (869 nt), except in clone  $\gamma$ -2, which exhibited two fragments (Fig. 2C). Upon nucleotide sequencing, except in clone  $\gamma$ -4 which had a deletion of four nucleotides

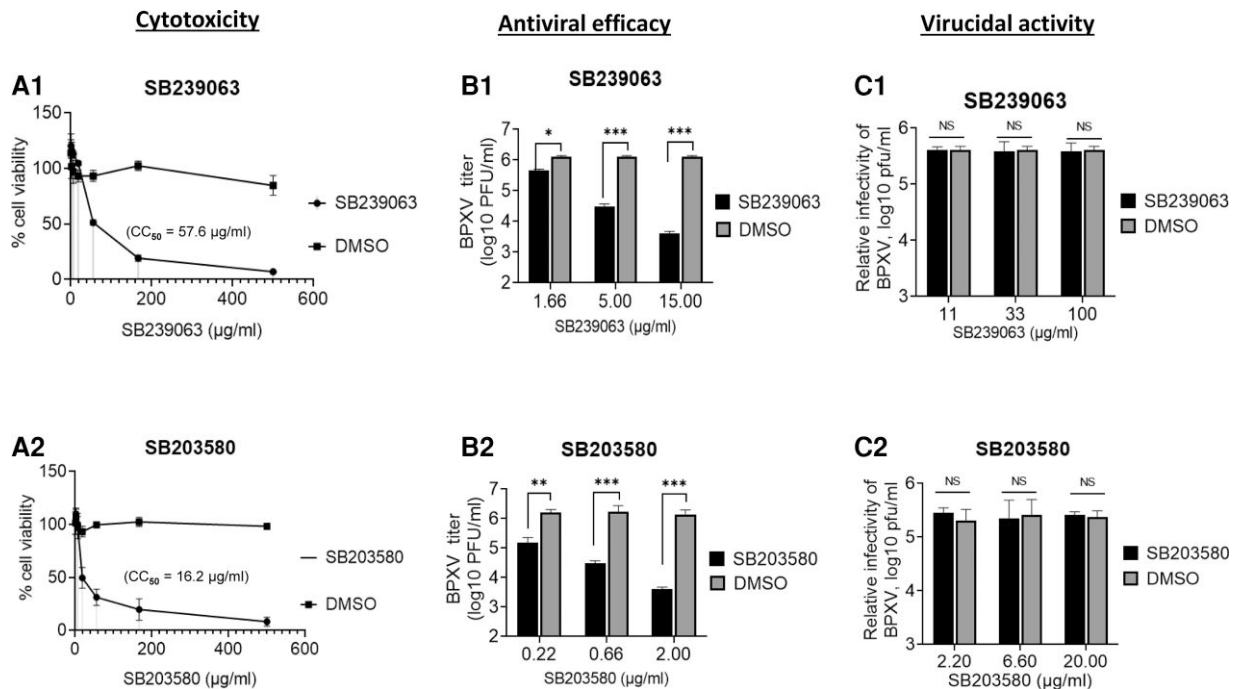


**Fig. 1.** p38 inhibition suppresses BPXV replication. (A) Determination of the cytotoxicity (MTT assay). Indicated concentrations of SB239063, SB203580 or equivalent volumes of DMSO, in triplicates, were incubated with cultured Vero cells for 96 h and percentage of the cell viability was measured by MTT assay.  $CC_{50}$  was determined by Reed-Muench method. (B) In vitro antiviral efficacy. Vero cells, in triplicates, were infected with BPXV at MOI of 0.1 in the presence of indicated concentrations of SB239063, SB203580 or equivalent volumes of DMSO. At 48 hpi, infectious virus particles released in the infected cell culture supernatants were quantified by plaque assay. (C) Virucidal activity. Indicated concentrations of the SB239063, SB203580 or equivalent volumes of DMSO, in triplicates, were mixed with BPXV ( $10^6$  PFU) and incubated for 90 min at 37 °C after which the virus was diluted (1/1000) and the residual viral infectivity was determined by plaque assay.

(1311–1314) and was kept for further studies, others were identical to WT Vero cells and hence discontinued (Fig. 2D).

The disruption of p38- $\alpha$  and p38- $\gamma$  in KO cells was further confirmed by Western blot analysis. Both p38- $\alpha$  and p38- $\gamma$  were detectable in WT Vero (Fig. 2E and 2F) cells, but not in the respective KO cells (Fig. 2E and 2F). Furthermore, p38- $\gamma$  and p38- $\alpha$  were detectable in p38- $\alpha$  KO and p38- $\gamma$  KO cells respectively (Fig. 2E and 2F) which confirmed that p38- $\gamma$  is intact in p38- $\alpha$  KO cells and p38- $\alpha$  is intact in p38- $\gamma$  KO cells.

### p38 MAPK Supports BPXV replication

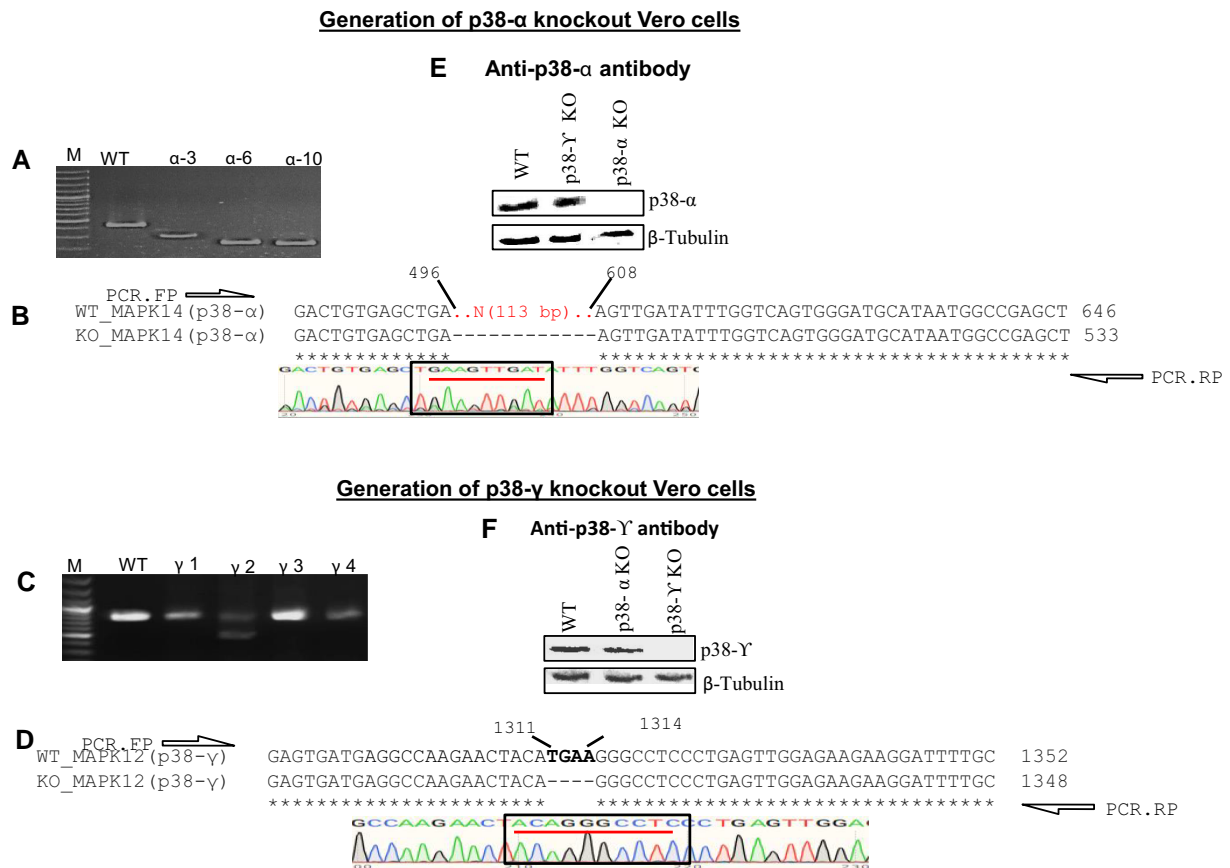
In order to further ascertain that the inhibitory effect of SB239063 on BPXV replication is due to p38- $\alpha$  inhibition and not due to the “off target” effects, we measured the yields of BPXV in WT- and p38- $\alpha$  knockout Vero cells. Lower yield of BPXV in p38- $\alpha$  knockout Vero cells as compared to the WT Vero cells (Fig. 3) suggested that p38 serves as a host-dependency factor for BPXV.

### p38 Inhibition Impairs BPXV Replication at Post-entry Steps

In order to examine which specific step(s) of BPXV life cycle could be affected by SB239063, initially, a time-of-addition assay was performed in the setting of one-step growth curve. Vero cells were infected with BPXV, and the SB239063- or DMSO were applied at a timely interval from 1 hour

post-infection (hpi) to 30 hpi. The yields of infectious virus in the infected cell culture supernatant were quantified when one full cycle of the BPXV was likely to be completed, i.e., at 36–48 hpi (Khandelwal et al. 2017). The application of SB239063 resulted in almost similar levels of BPXV inhibition, either applied before infection (pre-treatment) or at 1 hpi and 6 hpi (supplementary fig. S1, Supplementary Material online), suggesting that SB239063 does not inhibit early steps of BPXV life cycle (i.e., entry and attachment). The addition of inhibitor at later time points exhibited low (18hpi) or no inhibition (30 hpi), suggesting that SB239063 has no significant effect on the late stages of the BPXV life cycle (i.e., assembly/release of viruses). However, the addition of SB239063 between 6 and 18 hpi resulted in a significant reduction in the virus yield, thereby suggesting that SB239063 may target the post-entry but pre-budding stages of BPXV life cycle.

In order to determine the effect of SB239063 on the attachment of the BPXV to host cells, virus infection was carried out at 4 °C; it allowed attachment of the virus to the host cells but restricted viral entry. As indicated in supplementary fig. S2A, Supplementary Material online, viral titres were comparable in both DMSO-treated and SB239063-treated cells, implying that SB239063 does not affect BPXV attachment to the host cells. Besides, in order to evaluate the effect of SB239063 upon BPXV entry, the virus was first allowed to attach at 4 °C in the absence of inhibitor followed by incubation of the cells at 37 °C for 1.5 h (it allowed viral entry) in the presence of inhibitor. Viral titres after completion of one full



### p38- $\alpha$ KO Vero cells

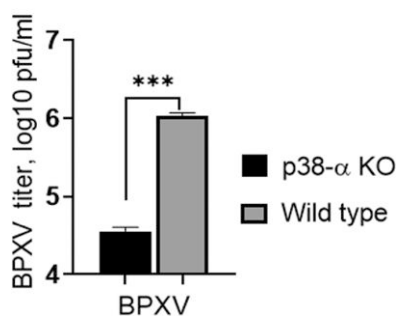


**Fig. 3.** p38 supports BPXV replication. Confluent monolayers of WT and p38- $\alpha$  KO Vero cells, in triplicates, were infected with BPXV at MOI of 0.1. The virus particles released in the infected cell culture supernatants at 48 hpi were quantified by plaque assay. Error bars indicate SD. Pair-wise statistical comparisons were performed using Student's *t*-test. (\*\*\*) =  $P < 0.001$ ). Values are means  $\pm$  SD and representative of the result of at least 3 independent experiments.

cycle (~36 hpi), were comparable in both DMSO-treated and SB239063-treated cells ([supplementary fig. S2B, Supplementary Material](#) online), suggesting that p38 inhibitor does not affect BPXV entry into the target cells. In the virus release assay, the inhibitor was applied at the time when early (attachment/entry) and middle stages (genome and protein synthesis) of the viral life cycle had occurred and when the virus presumably started to release from the infected cells (~at 36 hpi). Viral titres were comparable in both DMSO-treated and SB239063-treated cells ([supplementary fig. S2C, Supplementary Material](#) online), suggesting that p38 inhibitor does not affect BPXV release from the infected cells.

### p38 Inhibition Suppresses Levels of Viral Proteins and DNA in the Infected Cells

In order to determine the effect of SB239063 on the synthesis of viral proteins, Vero cells were infected with BPXV at a multiplicity of infection (MOI) of 5 and the



inhibitor was applied at 4 hpi, a time point wherein early steps of the viral replication cycles (attachment/entry) were expected to have occurred. As shown in Fig. 4A1 and A2, addition of SB239063 resulted in reduced BPXV protein synthesis without affecting the housekeeping control proteins. The reduced protein levels (viral polymerase), in turn, could impair BPXV DNA synthesis as well. Indeed, SB239063 was also shown to significantly decrease (~60%) viral DNA levels in the infected cells (Fig. 4B).

### BPXV Induces Biphasic Activation of p38 in Vero Cells

In order to examine whether BPXV induces activation of p38, cell lysates collected at various times post-infection, were probed for phosphorylated p38 (p-p38). The levels of total p38 and housekeeping control protein  $\beta$ -actin were static during the course of BPXV life cycle (Fig. 5A1) but those of p-p38 were found to be significantly higher at 2–4 hpi and 20–24 hpi (Fig. 5A1 and 5A2) as compared to the other time points examined. This suggested that BPXV induces biphasic activation of p38.

### p38 Inhibition Suppresses BPXV Replication by Targeting p38–MNK1–eIF4E Signaling Pathway

Like in several other viruses, BPXV also exploits the cap-dependent mechanism of protein translation (Kumar et al. 2018a; Khandelwal et al. 2020). This involves phosphorylation of eukaryotic translation initiation factor 4E

(p-eIF4E) which binds with the 5' cap of viral mRNA to facilitate initiation of translation. Several upstream kinases including p38 may activate eIF4E (Nagaleekar et al. 2011); therefore, we evaluated the levels of p-eIF4E in BPXV infected cells. The kinetics of eIF4E activation overlapped with p38 activation kinetics, as peak levels of p-eIF4E were also observed at 2–4 hpi and 20–24 hpi (Fig. 5A1 and 5A3). The treatment of SB239063 not only resulted in the reduction of p-p38 levels (Fig. 5B1 and 5B2) but also p-eIF4E (Fig. 5B1 and 5B3).

Phosphorylation of eIF4E by p38 MAPK is mediated via MNK1 which is a highly conserved mechanism in most cell types (Shveygert et al. 2010; Pashenkov et al. 2017; Mihail et al. 2019; Chander et al. 2021). Like p38 inhibition, a non-cytotoxic concentration of CGP57380 (MNK1 inhibitor) and 4EGI-1 (eIF4E inhibitor) also resulted in the reduction of BPXV yield in Vero cells (Fig. 6A and 6B) which suggests that BPXV exploits p38-MNK1-eIF4E signaling axis to effectively replicate in the target cells.

### p38 Inhibition Suppresses Binding of BPXV mRNA with eIF4E

In order to evaluate the interaction between eIF4E and BPXV mRNA, which is essential for translation of BPXV proteins, we conducted a chromatin immunoprecipitation (CHIP) assay. As shown in Fig. 6C, the amount of viral mRNA immunoprecipitated by  $\alpha$ -p-eIF4E was significantly lower in cells treated with SB239063 or 4EGI-1, as compared to the DMSO-treated cells. Since there was no detectable viral mRNA immunoprecipitated by  $\alpha$ -ERK (nonreactive antibody) and beads control (Fig. 6C), it was concluded that  $\alpha$ -p-eIF4E specifically binds to BPXV mRNA. Taken together, it was concluded that BPXV induces p38 cell signaling pathway and that this enhanced cell signaling activity is exploited by the virus to effectively synthesize viral proteins.

### Selection of Potential SB239063-resistant Mutants on Long-term in vitro Culture

In order to evaluate the development of drug-resistant BPXV variants, BPXV was serially passaged (P) 60 times in the presence of SB239063 or DMSO. No significant resistance was observed up to P30 but P40 virus showed significant resistance (Fig. 7A). However, a complete resistance could not be seen even up to P60 (Fig. 7A). At P60, BPXV-P60-SB239063 and BPXV-P60-Control, together with the original virus (BPXV-P0) were evaluated for their sensitivity to SB239063. The magnitude of the suppression of virus yield in SB239063-treated cells was lesser (~6-fold) in BPXV-P60-SB239063 infected as compared to BPXV-P0 or BPXV-P60-Control infected cells (~100-fold), suggesting the selection of resistant mutants by SB239063 (Fig. 7B). Similarly, as compared to BPXV-P0 and BPXV-P60-Control, BPXV-P60-SB239063 virus also replicated at higher titres in p38- $\alpha$  KO cells (Fig. 7C), which further indicated the development of resistant mutations in BPXV-P60-SB239063.

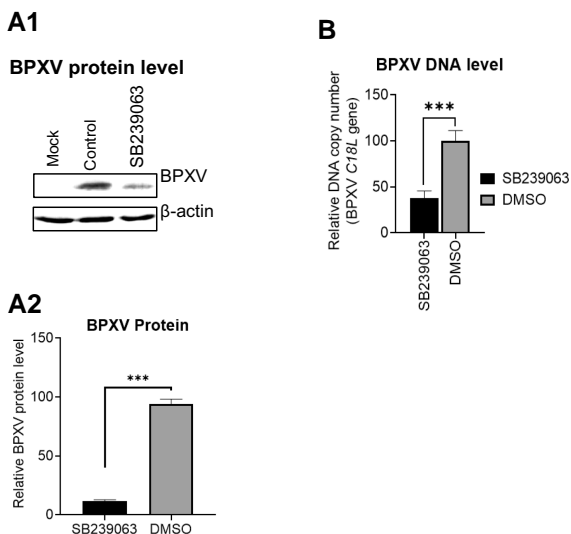


**Fig. 4.** p38 inhibitor impairs BPXV genome and protein synthesis. Confluent monolayers of Vero cells were infected with BPXV at an MOI of 5. The inhibitor or DMSO was applied at 3 hpi and the cells were scrapped at 24 hpi to examine the levels of viral proteins (A1). The blots were quantified by densitometry (ImageJ) and the data are presented as mean with SD. Histogram A2 shows band intensities of BPXV protein in inhibitor-treated and untreated cells. The levels of viral DNA is also shown (B). Pair-wise statistical comparisons were performed using Student's *t*-test. \*\*\* =  $P < 0.001$ . Values are means  $\pm$  SD and representative of the result of at least three independent experiments.

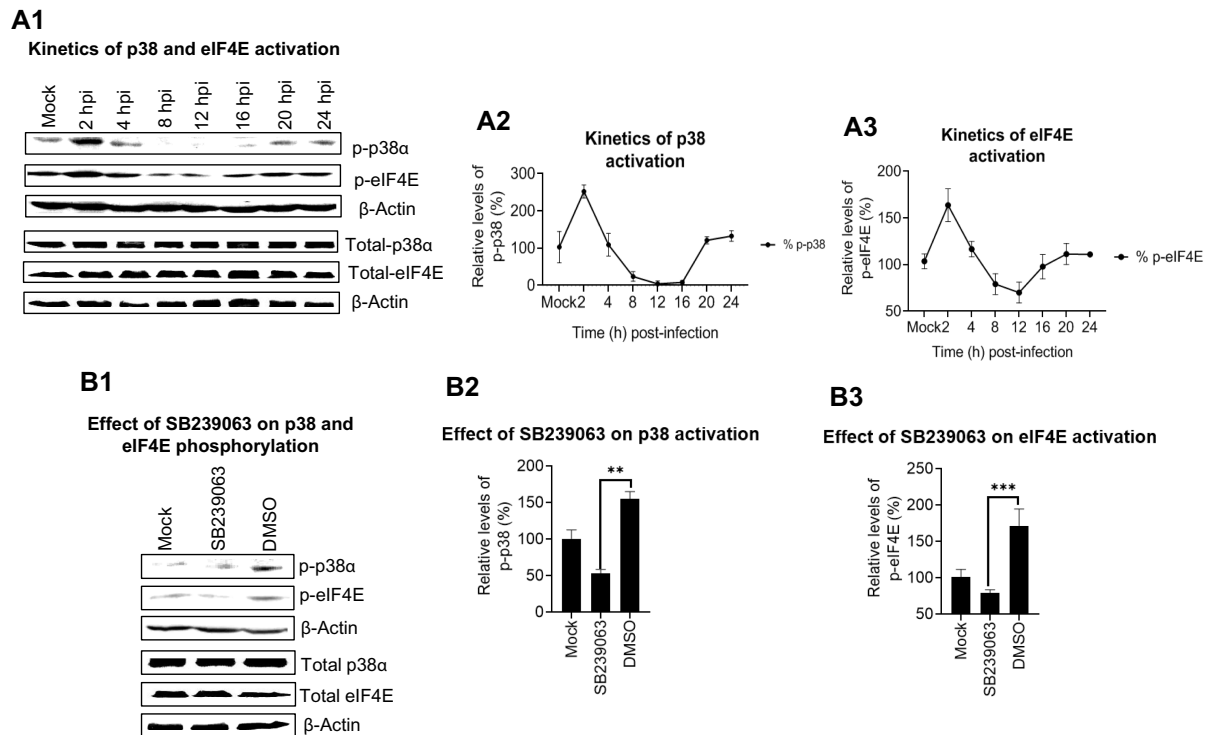


**Fig. 5.** (A) BPXV infection induces phosphorylation of p38 and eIF4E. Confluent monolayers of Vero cells were mock-infected (uninfected) or infected with BPXV at an MOI of 5. Cells were scraped at indicated time points. The levels of indicated cellular proteins as determined by Western blot analysis (A1) are shown. The blots were quantified by densitometry (ImageJ) and the data are presented as mean with SD. The histograms A2 and A3 show band intensity of p-p38 $\alpha$  and p-eIF4E levels, respectively (normalized with  $\beta$ -actin).  $n = 3$  independent experiments. (B). SB239063 blocks p38/eIF4E signaling. Confluent monolayers of Vero cells were infected with BPXV at an MOI of 5. Inhibitor or DMSO was applied at 3 hpi. Cells were scraped at 24 hpi and levels of the total- and phosphorylated form of p38 and eIF4E were determined by Western blot analysis (B). The blots were quantified by densitometry (ImageJ) and the data are presented as mean with SD. The histograms B2 and B3 show band intensities of p-p38 $\alpha$  and p-eIF4E in inhibitor-treated and untreated cells respectively.  $n = 3$  independent experiments.

### Resistant Virus Preferentially Utilize p38- $\gamma$

In order to examine whether BPXV-P60-SB239063 switches to use alternate cellular factor under long-term restricted availability of p38- $\alpha$ , we compared the growth of P0, P60-SB239063 and P60-Control viruses in WT, p38- $\alpha$  KO and p38- $\gamma$  KO cells (Fig. 8A). P0 virus replicated at  $\sim$ 50-fold lower titres in p38- $\alpha$  KO cells whereas marginal inhibition ( $\sim$  3-fold) was seen in p38- $\gamma$  KO cells as compared to the WT cells, which suggests that WT BPXV is highly dependent on p38- $\alpha$  with a very low requirement of p38- $\gamma$  (Fig. 8B). Likewise, P60-Control virus also replicated at  $\sim$ 75-fold lower titres in p38- $\alpha$  KO cells but had a marginal inhibition ( $\sim$ 5-fold) in p38- $\gamma$  KO cells (Fig. 8C). However, resistant virus (P60-SB239063) replicated more efficiently in the presence of p38- $\gamma$  as compared to p38- $\alpha$  because virus yields were  $\sim$ 4-fold lower in p38- $\alpha$  KO and  $\sim$ 20-fold lower in p38- $\gamma$  KO cells (Fig. 8D). Thus, it was concluded that WT BPXV (P0) is dependent on p38- $\alpha$ , which under long-term selective pressure of p38 inhibitor generates mutants (P60-SB239063) that preferentially use p38- $\gamma$  instead of p38- $\alpha$ .

### Analysis of Resistance-associated Mutations in the Viral Genome

Nucleotide sequences of the wild type virus (BPXV P0) were previously deposited by our team in the NCBI GenBank

with an Accession Number MW883892.1. Whole genome sequences of BPXV-P60-SB239063 and BPXV-P60-Control viruses are deposited in NCBI GenBank with Accession Numbers of ON974728 and ON974727, respectively. In order to identify resistance-associated (SB239063-resistant) mutations, we compared the genome of BPXV-P60-SB239063 and BPXV-P60-Control viruses. Two unique mutations, one non-synonymous mutation (C201Y) in the coding region of Ribonucleoside-diphosphate reductase (Fig. 9A and 9B) and one point mutation (C-A) in the promoter region of Ser/Thr kinase (Fig. 9C) were identified in BPXV-P60-SB239063 as compared to BPXV-P60-Control. These mutations were not found in other sequences available in the public domain (supplementary table S1, Supplementary Material online).

Seven frameshifts, one deletion, and one point mutation were present in both BPXV-P60-SB239063 and BPXV-P60-Control as compared to P0 virus. These could be potentially associated with the adaptation of the virus in the cell culture due to high sequential passage (Fig. 9A). One non-synonymous mutation (H159N) in Poly A polymerase catalytic subunit was exclusively present in BPXV-P60-Control virus as compared to P0 or P60-SB239063 virus (supplementary table S1, Supplementary Material online).

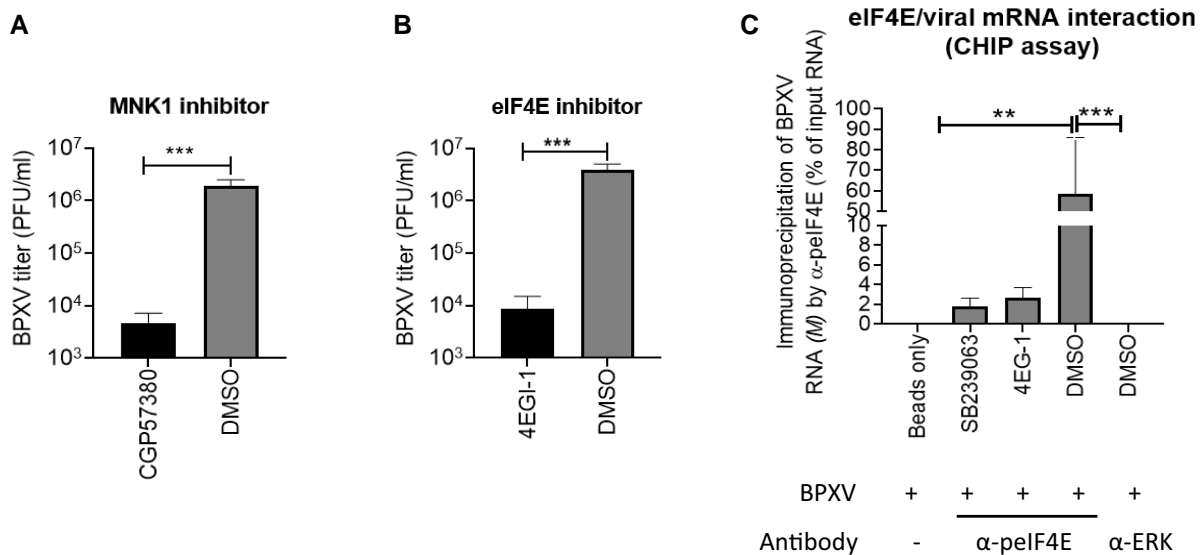


**Fig. 6.** p38 mediates BPXV mRNA translation by regulating p38–MNK1–eIF4E signaling axis. (A/B) MNK1 and eIF4E inhibition suppresses BPXV replication. Vero cells, in triplicates, were infected with BPXV at MOI of 0.1 in the presence of 1  $\mu$ g/mL of CGP57380 (MNK1 inhibitor), 2  $\mu$ g/mL 4EGI-1 (eIF4E inhibitor) or equivalent volumes of DMSO. At 48 hpi, infectious virus particles released in the infected cell culture supernatants were quantified by plaque assay. Reduction in viral yields in the presence of CGP57380 (A) and 4EGI-1 (B) is shown. (C) p38 inhibition blocks binding of the viral mRNA with eIF4E (CHIP assay): Vero cells were infected with BPXV at MOI of 5. At 6 hpi, the cells were treated with SB239063, CGP57380 (MNK1 inhibitor) or DMSO. At 16 hpi, cell lysates were prepared as per the procedure described for CHIP assay (materials and method section). The clarified cell lysates were incubated with  $\alpha$ -eIF4E (reactive antibody),  $\alpha$ -ERK (nonreactive antibody) or equivalent volume of IP buffer (Beads control), followed by incubation with Protein A Sepharose slurry. The beads were then washed five times in IP buffer. To reverse the cross-linking, the complexes were then incubated with Proteinase K. Finally, the reaction mixtures were centrifuged and the supernatant was subjected to cDNA preparation and quantitation of BPXV RNA (M gene) by qRT-PCR. Error bars indicate SD. Pair-wise statistical comparisons were performed using Student's t-test (\*\*=  $P < 0.01$ ). Values are means  $\pm$  SD and representative of the result of at least 3 independent experiments.

### Antiviral Efficacy of SB239063 in Providing Protection to Embryonated Chicken Eggs Against Lethal BPXV infection

Members of the family *Poxviridae* can infect chicken embryos and cause distinctly visible lesions (pocks) on chorio-allantoic membrane (CAM) of the embryonated chicken eggs (Baxby 1969; Marennikova et al. 1973). We exploited this model to evaluate the *in-ovo* efficacy of SB239063 against BPXV. Mortality of the embryos was observed at SB239063 concentration  $\geq 20$   $\mu$ g/egg, but not at 4  $\mu$ g/egg (Fig. 10A). The LD<sub>50</sub> was determined to be 29.90  $\mu$ g/egg. For evaluation of anti-BPXV efficacy of SB239063, eggs were infected with BPXV at 100 EID<sub>50</sub> along with three different concentrations (10  $\mu$ g/egg, 5  $\mu$ g/egg and 2.5  $\mu$ g/egg) of SB239063. SB239063 provided protection from the BPXV-associated mortality in a dose-dependent manner (Fig. 10B). The EC<sub>50</sub> was determined to be 4.20  $\mu$ g/egg. As compared to the DMSO (control), no obvious pock lesions could be observed in SB239063 inoculated eggs (protected groups) (Fig. 10C). Taken together, it was concluded that SB239063 prevents the development of BPXV-induced pock lesions on CAM, as well as the associated mortality.

### Discussion

Viruses rapidly develop drug-resistant variants, therefore, developing antiviral therapeutics is a major challenge (Kumar et al. 2011b; Pawlotsky 2012; Kumar et al. 2014;

Chaudhary et al. 2015). MAPKs play key roles in several cellular processes such as cell proliferation, differentiation, transformation and apoptosis. Mammals express at least four distinctly regulated groups of MAPKs which include ERK-1/2, p38 proteins, Jun amino-terminal kinases (JNK1/2/3) and ERK5. Activated p38 further induces activation of several transcription factors/effector proteins which eventually regulate several cellular processes such as cell cycle, apoptosis, cytoskeleton remodeling as well as inflammatory and immune responses (Han et al. 2020; Chander et al. 2021). A wide variety of viruses are known to directly interact with different isoforms of p38 or their substrates during replication (Marchant et al. 2009; Mikkelsen et al. 2009; Peng et al. 2014; Su et al. 2017; Nayak et al. 2019; Datta et al. 2021; Higgins et al. 2021; Mudaliar et al. 2021; Sugasti-Salazar et al. 2021). While some of the interactions are pro-viral (Zachos et al. 1999; Adamson et al. 2000; Marchant et al. 2009; Mikkelsen et al. 2009; Skaug and Chen 2010; Nagaleekar et al. 2011; Peng et al. 2014; Su et al. 2017; Kumar et al. 2018b; Nayak et al. 2019; Datta et al. 2021; Higgins et al. 2021; Mudaliar et al. 2021; Sugasti-Salazar et al. 2021), others suppress virus yield (Penrose et al. 2004; Schuck et al. 2013; Wei et al. 2013). Some viruses may subvert p38 functions to effectively replicate inside cells (Halfmann et al. 2011; Chen et al. 2017).

In order to examine the role of p38 signaling in BPXV infections, initially p38-specific inhibitors (SB239063 and SB203580) were employed. The reduction in the virus yield

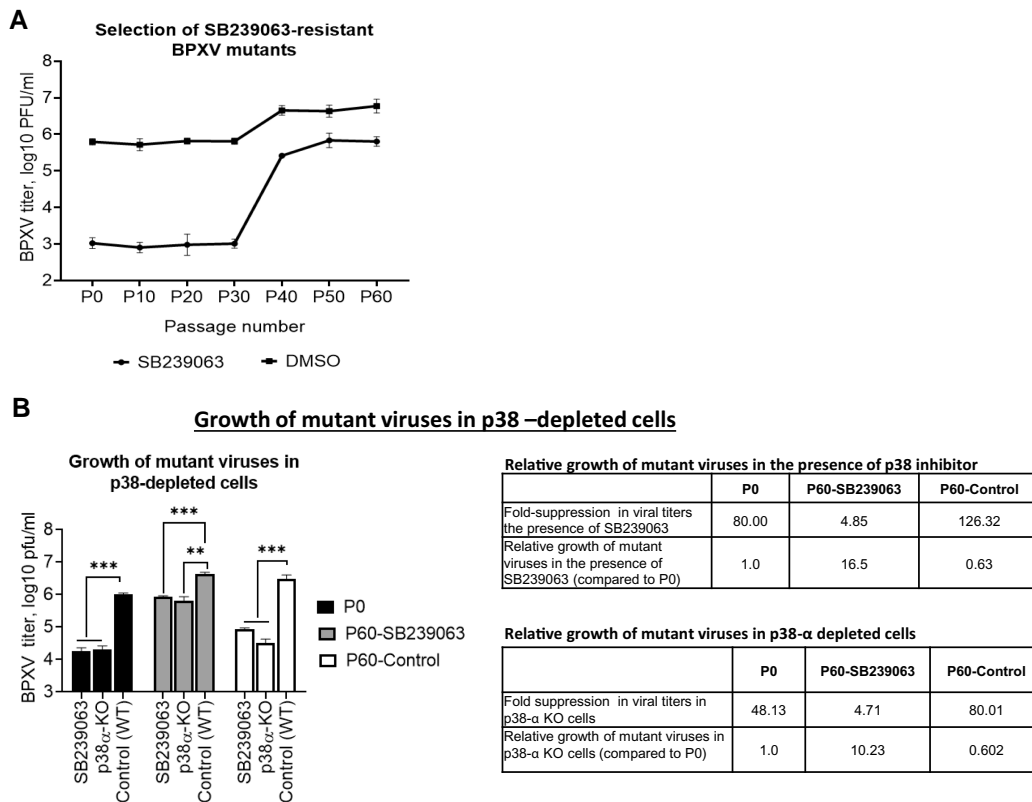


**Fig. 7.** Selection of potential SB239063-resistant mutants. (A) Long-term *in vitro* culture of BPXV in the presence of SB239063. BPXV was sequentially passaged in Vero cells in the presence of 5  $\mu\text{g}/\text{mL}$  SB239063 or equivalent volume of DMSO. At each passage, the confluent monolayers of Vero cells were infected with the virus, washed 5 times with PBS before a fresh aliquot of MEM was added and incubated for 48–96 h or until the appearance of cytopathic effect in  $\geq 50\%$  cells. The virus released in the supernatant was termed as passage 1 (P1) and used in the second round of infection, which was termed as P2. Virus at P0, P10, P20, P30, P40, P50 and P60 was evaluated for its sensitivity to SB239063. (B) Relative growth of BPXV-P0, BPXV-P60-SB239063 and BPXV-P60-Control in p38-depleted cells. Confluent monolayers of WT or p38- $\alpha$  KO Vero cells were infected with the indicated viral variants at MOI of 0.1 for 1 h. Following washing, WT Vero cells were treated with either SB239063 (10  $\mu\text{g}/\text{mL}$ ) or equivalent volume of DMSO. The yields of infectious progeny virus particles at 48 hpi were determined by plaque assay. Relative growth of mutant viruses in p38-depleted cells (inhibitor-treated and p38- $\alpha$  KO cells) is also shown in the right panel. Error bars indicate SD. Pair-wise statistical comparisons were performed using Student's *t*-test. (\*\*\*) =  $P < 0.001$ ). Values are means  $\pm$  SD and representative of the result of at least three independent experiments.

in p38 inhibitor (SB239063 and SB203580)-treated and p38 $\alpha$ -knockout Vero cells suggested that p38 MAPK signaling is a prerequisite for BPXV replication. Further, we also demonstrated that SB239063 inhibitor-mediated suppression of BPXV replication is primarily due to the reduced levels of viral proteins and moderately due to low levels of DNA but without any significant effect on viral attachment, entry, and budding. Our findings are in agreement with previous studies on other viruses wherein p38 has been shown to facilitate the synthesis of viral proteins (Banerjee et al. 2002; Cook 2016; Su et al. 2017; Zhan et al. 2020; Higgins et al. 2021; Mudaliar et al. 2021; Sugasti-Salazar et al. 2021). However, p38 also supports RNA synthesis [respiratory syncytial virus (RSV) and influenza A virus (Choi et al. 2016)] and viral assembly [HCV (Cheng et al. 2020)] which seems to be due to the involvement of different downstream molecules (Cuadrado and Nebreda 2010; Chander et al. 2021).

Upon activation, p38 may regulate activity of several effector proteins (transcription factors) which eventually

modulate several viral and cellular events including translation of viral proteins (Chander et al. 2021). Like several other viruses, BPXV also exploits the cap-dependent mechanism of protein translation (Kumar et al. 2018a; Khandelwal et al. 2020). This involves phosphorylation of eIF4E (p-eIF4E) which binds with the 5' cap of viral mRNA to facilitate initiation of protein translation (Kumar et al. 2018a; Khandelwal et al. 2020). We observed that BPXV induces biphasic activation (phosphorylation) of p38- $\alpha$ . The kinetics of p38- $\alpha$  phosphorylation overlapped with eIF4E phosphorylation. In addition, both p38- $\alpha$  and eIF4E activation could be blocked by SB239063. This tempted us to speculate that low levels of BPXV proteins in SB239063-treated cell could be the result of the inhibition of viral protein synthesis.

p38 may be activated by several upstream kinases (Chander et al. 2021). In most instances, p38 MAPK is targeted by MKK3 and MKK6 (Stramucci et al. 2018). MKK3 preferentially targets the p38- $\alpha$  and p38- $\beta$ , whereas MKK6 can activate all p38 isoforms (Yang et al. 2010). Activated



**A**

	Viral titres PFU/ml (Mean ± SD)		
	BPXV P0	BPXV P60-Control	BPXV P60-SB239063
p38- $\alpha$ KO cells	21333 ± 4618	40000 ± 4000	906666 ± 66533
p38- $\gamma$ KO cells	373333 ± 61101	520000 ± 105830	217333 ± 50013
WT cells	1026666 ± 100664	3200000 ± 800000	4266666 ± 61101

**Fold suppression of viral titers in p38- $\alpha$  KO and p38- $\gamma$  KO cells (compared to WT cells)**

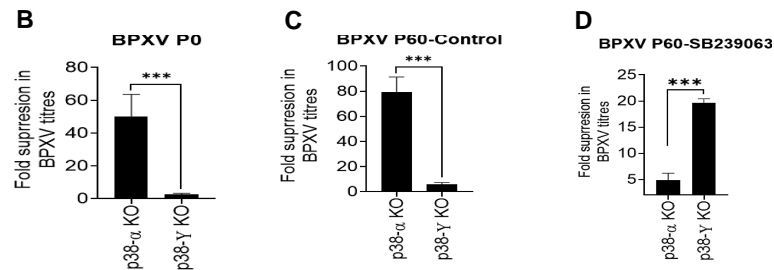


**FIG. 8.** Resistant virus switches its preference to utilize p38- $\gamma$ . p38- $\alpha$  KO, p38- $\gamma$  KO or WT Vero cells, in triplicates, were infected with BPXV P0, BPXV-P60-SB239063 or BPXV-P60-Control viruses at an MOI of 0.1. Infectious progeny virus particles released at 48 hpi were quantified by plaque assay (A). The viral titers were further analyzed to determine fold-suppression in KO cells (p38- $\alpha$  KO or p38- $\gamma$  KO) as compared to the WT Vero cells. Fold suppression of P0 (B), P60-Control (C) and P60-SB239063 (D) virus is shown. Error bars indicate SD. Pair-wise statistical comparisons were performed using Student's *t*-test. (\*\*\*) =  $P < 0.001$ ). Values are means  $\pm$  SD and representative of the result of at least three independent experiments.

p38 MAPK phosphorylates MNK1 which in turn leads to the phosphorylation of eIF4E. This is the most conserved mechanism of eIF4E phosphorylation in most cell types (Shveygert et al. 2010; Pashenkov et al. 2017; Mihail et al. 2019; Chander et al. 2021). We demonstrated that similar to p38, MNK1 and eIF4E-inhibition also results in the reduction of BPXV yield in Vero cells, which suggests that BPXV exploits the p38-MNK1-eIF4E signaling axis to effectively replicate in the target cells. Inhibition of viral mRNA and eIF4E interaction by both SB239063 and 4EGI-1 in CHIP assay further confirmed that p38-MNK1-eIF4E signaling is a prerequisite for translation of viral proteins (Fig. 11).

Whereas direct virus-acting antiviral agents are well known to rapidly induce drug-resistant phenotype (Kumar et al. 2011b), host-directed antiviral agents are less prone to induce the selection of drug-resistant phenotypes (Kumar et al. 2008; Kumar et al. 2011a; Chaudhary et al. 2015; Kumar et al. 2018a; Kumar et al. 2018b; Kumar et al. 2019; Kumar et al. 2020; Xu et al. 2020) because viruses cannot easily regain the missing cellular factors by mutation (Kumar et al. 2018b; Kumar et al. 2020). However, emerging evidence suggests that resistance to host-directed antiviral agents can indeed occur at a relatively low level upon long-term restricted availability of the targeted cellular factor (Hopcraft and Evans 2015). In order to select SB239063-resistant virus variants, BPXV was serially passaged 60 times in the presence or absence of SB239063. As compared to the P60-Control, P60-SB239063 virus replicated at significantly higher titres in SB239063-treated cells, suggesting the emergence of SB239063-resistant BPXV mutants. After HIV-1 resistance against Maraviroc (CCR5 antagonist) (Ratcliff et al.

2013), this is a rare evidence wherein a virus was shown to develop drug resistance against a host-directed antiviral agent.

On the basis of amino-acid sequence identity, p38 MAPK subfamily is divided into two distinct subsets. The first group consists of p38- $\alpha$  and p38- $\beta$ , while the other p38- $\gamma$  and p38- $\delta$ . p38 inhibitors such as SB203580, SB202190 and SB239063 can inhibit p38- $\alpha$  and p38- $\beta$  but p38- $\gamma$  and p38- $\delta$  remain completely unaffected (Cuenda et al. 1997; Kumar et al. 1997; Kuma et al. 2005; Cuenda and Rousseau 2007). Although not yet fully understood, there are examples wherein the virus can either switch to use alternate host factor(s) (Hopcraft and Evans 2015) or alter its affinity towards the HDF(s) to become resistant (van der Linden et al. 2015; Bauer et al. 2017; Kumar et al. 2020). In order to evaluate whether BPXV switches to use an alternate host factor/analog/isoform, we generated p38- $\alpha$  and p38- $\gamma$  KO cells by CRISPR/Cas9-mediated genome editing. It was demonstrated that unlike the original virus (P0) and P60-Control virus which were highly dependent on p38- $\alpha$  with a very low requirement of p38- $\gamma$ , the resistant virus (P60-SB239063) was highly dependent on the p38- $\gamma$  with a limited requirement of p38- $\alpha$  (Fig. 12), suggesting that the resistant virus has switched over to use alternate host factor. It appears that while p38- $\gamma$  serves as a major cellular factor, p38- $\alpha$ /p38- $\beta$ /p38- $\delta$  may have some accessory function in the life cycle of resistant BPXV. This is a rare evidence wherein virus was shown to bypass the dependency on a critical cellular factor under selective pressure of a drug, although, in a knockout cell model, long-term propagation of the HCV in CLDN1 (tight junction protein claudin-1) knockout cells was shown to generate viral mutants that were dependent on the

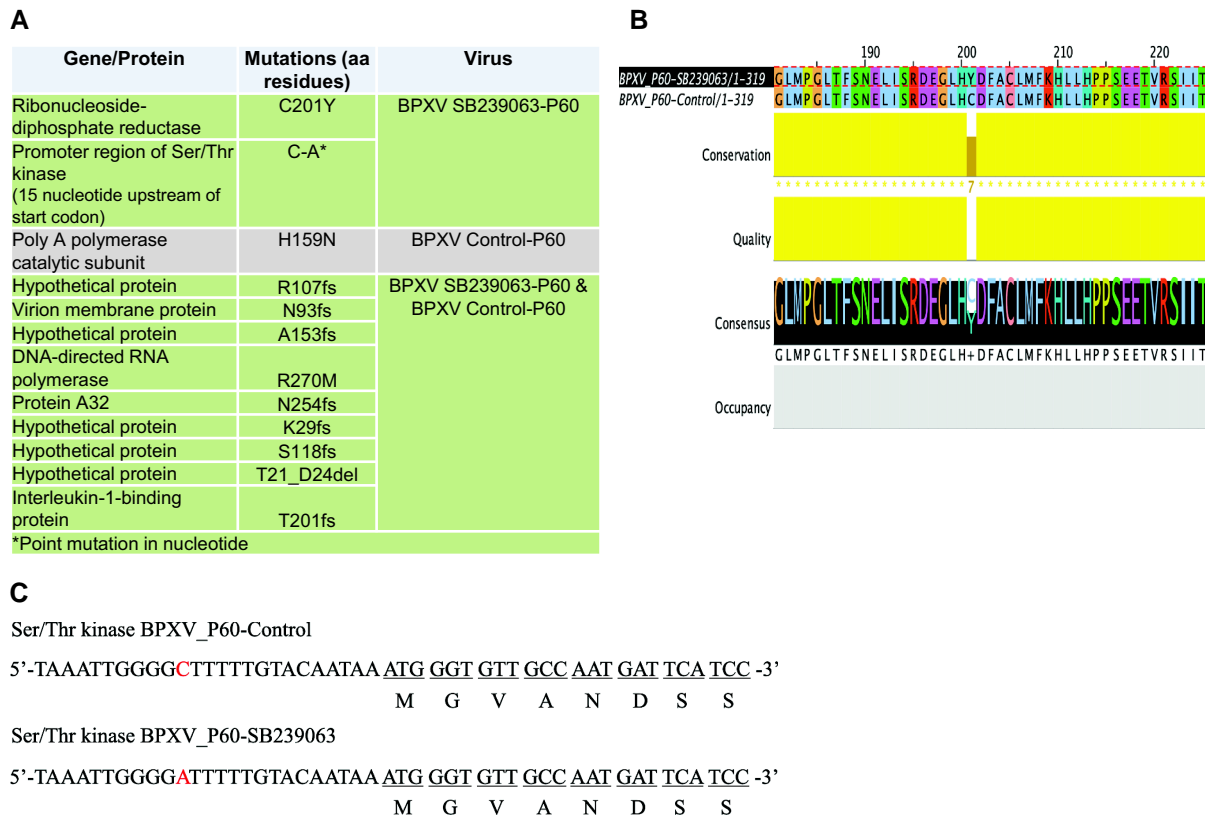


**Fig. 9.** Mutational analysis in BPXV-P60-SB239063 and BPXV-P60-Control viruses. Whole genome sequences of BPXV-P60-SB239063 and BPXV-P60-Control viruses were compared with BPXV P0 virus to identify the mutations in the passaged viruses (A). Resistance-associated (SB239063-resistant) mutations were identified by comparing the genome of BPXV-P60-SB239063 and BPXV-P60-Control. Two unique mutations, one nonsynonymous mutation (C201Y) in the coding region of Ribonucleoside-diphosphate reductase (B) and one point mutation (C-A) in the promoter region of Ser/Thr kinase (C) were identified in BPXV-P60-SB239063 as compared to BPXV-P60-Control.

CLDN6/CLDN9, rather than CLDN1 (Hopcraft and Evans 2015).

Generating a resistant virus that is completely dependent on p38- $\gamma$  along with studying the role(s) of other p38 isoform(s) in the life cycle of WT and resistant BPXV is essential and needs further investigation.

It was observed that both P60-Control and P60-SB239063 viruses grow ~10-fold faster than P0 virus (Fig. 7). We identified seven frameshifts, one deletion, and one point mutations in both BPXV-P60-SB239063 and BPXV-P60-Control as compared to P0 virus. These mutations could be associated with their high fitness, although there is a need for further investigation. We also mapped at least two resistance-associated mutations in BPXV P60-SB239063 genome, a nonsynonymous mutation (C201Y) in the coding region of Ribonucleoside-diphosphate reductase and a point mutation (C-A) in the promoter region of Ser/Thy kinase. Introducing these resistance-associated mutations in the backbone of WT BPXV with the help of reverse genetics system is essential to precisely understand the role of these mutations in acquiring viral resistance against SB239063, which is however beyond the scope of this study.

SB239063 also provided a significant therapeutic effect against lethal infection with BPXV in embryonated chicken eggs, suggesting its *in vivo* potential as an antiviral agent against poxvirus infections. Since host-directed agents

interfere with the host cell metabolism, their use is always associated with a risk of cytotoxicity. For example, PI4K $\beta$  inhibitors are known to exert potent antiviral activity against enteroviruses, but they may prove to be lethal in mice, preventing their further development as antiviral drugs (Lamarche et al. 2012). Therefore, further validation and *in vivo* efficacy of SB239063 are essential before actually introducing it from the research into the clinical settings.

In conclusion, p38- $\alpha$  serves as a critical cellular factor for the synthesis of BPXV proteins, and may serve as a novel target for antiviral drug development against buffalopox. BPXV does not easily select SB239063-resistant mutant. However, long-term selective pressure of SB239063 allows the virus to switch over to use p38- $\gamma$ , so as to become resistant against the p38- $\alpha$  inhibitor.

## Materials and Methods

### Chemicals

SB239063 (supplementary fig. S1a, Supplementary Material online) and SB203580 (supplementary fig. S1b, Supplementary Material online) (structurally related p38  $\alpha/\beta$  MAPK inhibitors), CGP57380 (MNK1 inhibitor), and 4EGI-1 (eIF4E inhibitor) were procured from Sigma (Steinheim, Germany). These inhibitors were dissolved in Dimethyl sulfoxide (DMSO), thereby DMSO was used as a vehicle control in the experiments.

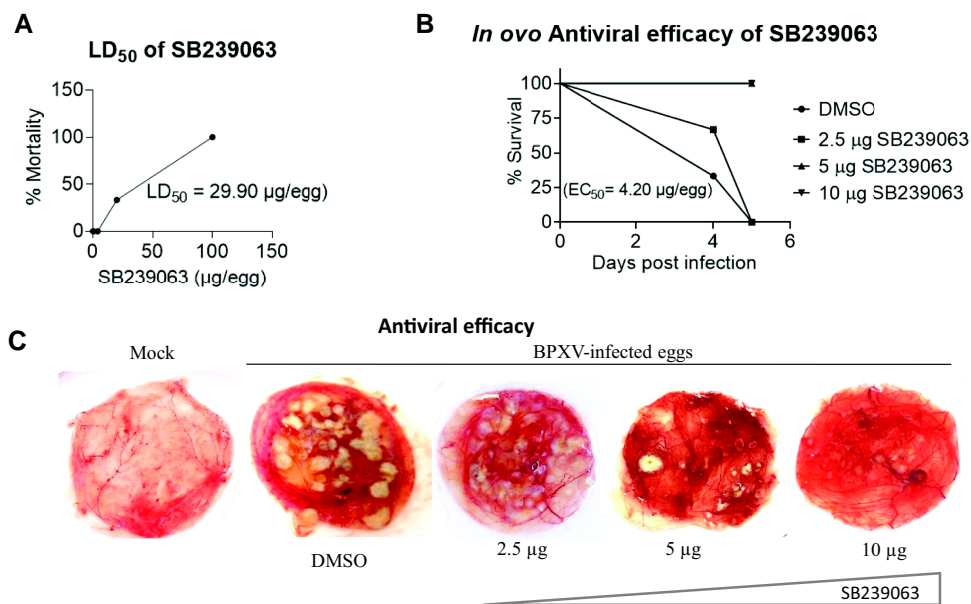


**FIG. 10.** *In ovo* antiviral efficacy of SB239063 against BPXV. (A) Determination of the LD<sub>50</sub> of SB239063. LD<sub>50</sub> was determined by inoculating 5-fold serial dilutions of SB239063 (concentration ranging from 100 to 0.16 µg/egg) in 10 days old embryonated SPF eggs, in a total of 100 µl volumes via CAM. Eggs were examined for the viability of the embryos up to five days post-inoculation to determine the LD<sub>50</sub> by the Reed-Muench method. (B) *In ovo* antiviral efficacy (EC<sub>50</sub>) of SB239063. SPF embryonated chicken eggs, in triplicates, were inoculated with 2-fold dilutions (10 to 2.5 µg/egg) of SB239063 or DMSO via CAM route, followed by infection with BPXV at 100 EID<sub>50</sub>. At 5 days post-infection, eggs were examined for pock lesions and/or death of the embryos. EC<sub>50</sub> was determined by the Reed-Muench method. The values are means ± SD and representative of the result of at least three independent experiments.

### Cell Culture

African green monkey kidney (Vero) cells were available at National Centre for Veterinary Type Cultures (NCVTC), Hisar. Cells were grown in Dulbecco's Modified Eagle's Medium (DMEM) supplemented with 5–10% fetal calf serum (FBS) (Sigma, St. Louis, USA) and antibiotics solution (Penicillin-Streptomycin).

### Virus

Vero cell adapted BPXV (Accession Number, VTCC-AVA90) was available at NCVTC Hisar. It was amplified and quantitated by plaque assay in Vero cells, as described previously (Khandelwal et al. 2017). The viral titers were determined as plaque forming units/mL (PFUs/mL).

### Antibodies

Mouse eIF4E monoclonal antibody (5D11), Rabbit anti-β-Tubulin primary antibody and Phospho-eIF4E (Ser209) polyclonal antibody were received from Invitrogen (South San Francisco, CA, USA). Rabbit p38 MAPK Antibody and rabbit p38-γ MAPK Antibody, were procured from Cell Signaling Technology (Massachusetts, USA). Mouse anti-β actin primary antibody, Anti-Mouse IgG (whole molecule)–Alkaline Phosphatase antibody (produced in goat) and Anti-Rabbit IgG (whole molecule)–Peroxidase antibody (produced in goat) were received from Sigma-Aldrich (St. Louis, USA). Hyperimmune serum that reacts with 15 KDa and 35 KDa BPXV proteins was raised in rabbits

and has been described earlier by our group (Khandelwal et al. 2017).

### Cytotoxicity and Virucidal Activity

For determination of the cytotoxicity, three-fold serial dilutions of SB239063, SB203580, or equivalent volumes of DMSO were incubated with Vero cells for 96 h and the cytotoxicity was determined by MTT assay as described previously (Kumar et al. 2008). Sub-cytotoxic concentration of CGP57380 (1 µg/mL) and 4EGI-1 (2 µg/mL) has been described elsewhere by our group (Kumar et al. 2018a; Khandelwal et al. 2020). For determination of the virucidal activity, aliquots of BPXV (~10<sup>6</sup> PFU each) were incubated with 3-fold serial dilutions of the inhibitor for 90 min. Thereafter, residual viral infectivity was determined by plaque assay (Kumar et al. 2011b).

### Time-of-addition Assay

Confluent monolayers of Vero cells, in triplicates were infected with BPXV at MOI of 5, followed by addition of SB239063 (10 µg/mL) or equivalent volume of DMSO at 1 hpi, 6 hpi, 12 hpi, 18 hpi, 24 hpi and 30 hpi. Supernatants from the infected cells were collected at 48 hpi and quantified by plaque assay.

### Attachment Assay

Confluent monolayers of Vero cells, in triplicates, were pre-incubated with 10 µg/mL of SB239063 or 0.05% DMSO for 30 min followed by BPXV infection at MOI of 5 for 2 h at 4 °

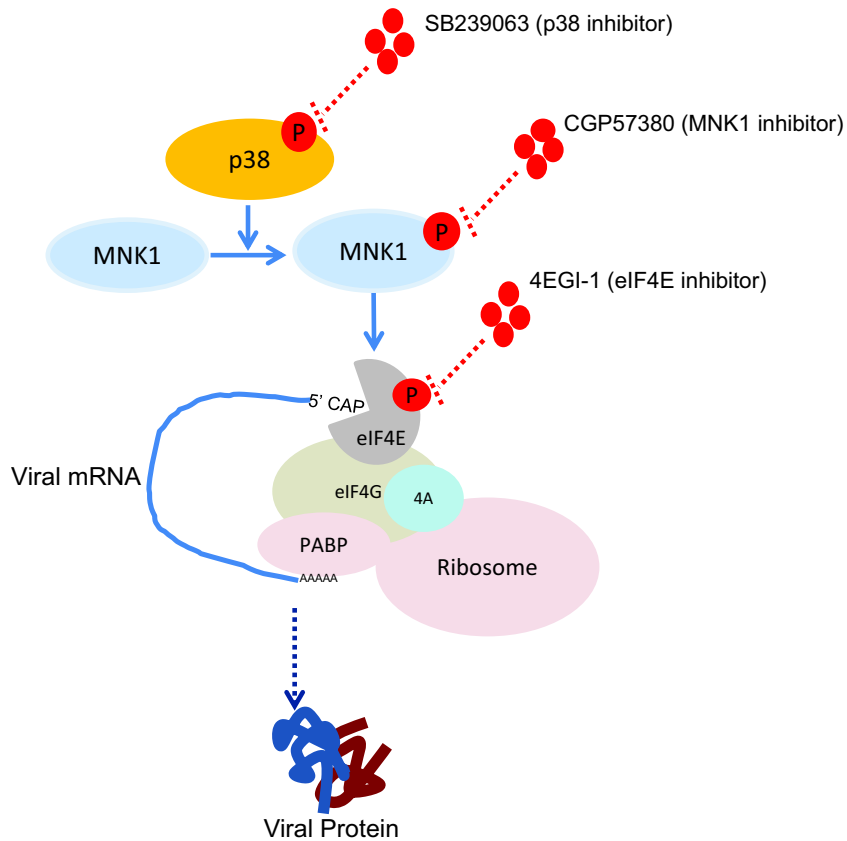


**Fig. 11.** p38-MNK1-eIF4E signaling axis regulates translation of BPXV proteins. BPXV induces phosphorylation of p38 MAPK. Activated p38 induces phosphorylation of MNK1 which eventually phosphorylates eIF4E. Phosphorylated eIF4E, in association with other translation initiation factors, interacts with the viral mRNA to initiate the translation of viral proteins. Disruption of p38/MNK1/eIF4E signaling by chemical inhibitors results in reduced synthesis of viral proteins, and thereby may serve as a target for antiviral drug development.

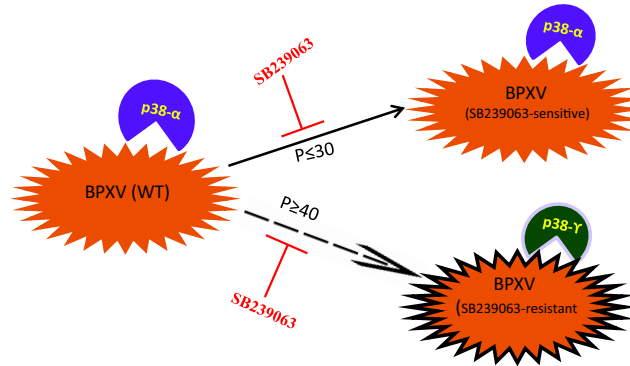


**Fig. 12.** BPXV switches to use p38- $\gamma$  under long-term selective pressure of p38- $\alpha$  inhibitor. p38- $\alpha$  MAPK is a critical cellular factor that positively regulates BPXV replication. Long-term sequential passage ( $P \geq 40$ ) of BPXV in Vero cells in the presence of p38- $\alpha$  inhibitor (SB239063) induces generation of viral mutants that preferentially utilize p38- $\gamma$  instead of p38- $\alpha$ , thereby becoming resistant against the targeting agent (SB239063).

C. The cells were then washed 5 times with PBS and the cell lysates were prepared by rapid freeze-thaw method. The viral titers in cell lysates were quantified by plaque assay.

### Entry Assay

Confluent monolayers of Vero cells, in triplicates, were pre-chilled at 4 °C and infected with BPXV at MOI of 5 in SB239063-free medium for 1.5 h at 4 °C, which allowed the virus attachment to the host cells but restricted viral entry. Thereafter, the cells were washed with PBS and incubated with fresh MEM containing 10  $\mu\text{g}/\text{mL}$  of SB239063 or 0.05% DMSO. To permit viral entry, cells were incubated at 37 °C for 1 h. The cells were then washed with PBS and

grown in fresh DMEM without any drug. Virus yield in the infected cell culture supernatants was determined by plaque assay at 48 hpi.

### Virus Release Assay

Confluent monolayers of Vero cells, in triplicates, were infected with BPXV at MOI of 5 for 1 h. Thereafter, cells were washed with PBS and fresh DMEM was added. At 36 hpi, cells were washed 5 times with chilled PBS followed by addition of fresh DMEM containing 10  $\mu\text{g}/\text{mL}$  SB239063 or equivalent volume of DMSO. Virus yield in the infected cell culture supernatant was quantified by plaque assay at 0.5 h and 2 h post-drug treatment.



### qRT-PCR

The amount of viral DNA/mRNA (cDNA) in infected cells was measured by quantitative real-time PCR (qRT-PCR). Confluent monolayers of Vero cells, in triplicates, were infected with BPXV (MOI of 5) for 1 h followed by washing with PBS and addition of fresh DMEM. SB239063 (10 µg/mL) or DMSO (0.05%) were added at 6 hpi. Cells were scraped at 36 hpi to quantify the viral (C18L) and housekeeping control gene ( $\beta$ -actin) by qRT-PCR as previously described (Khandelwal et al. 2017). The levels of viral DNA, expressed as threshold cycle (Ct) values, were normalized with  $\beta$ -actin housekeeping control gene. Relative fold-change in viral DNA copy number was determined by  $\Delta\Delta$  Ct method (Livak and Schmittgen 2001).

### Effect on the Synthesis of Viral Proteins

Confluent monolayers of Vero cells were infected with BPXV at MOI of 5. Inhibitors or DMSO were added at 6 hpi. Cells were scraped at 36 hpi to analyze the levels of viral and housekeeping control protein glyceraldehyde-3-phosphate dehydrogenase (GAPDH) in Western blot analysis. Anti-BPXV serum was available at NCVTC Hisar which has been described elsewhere (Khandelwal et al. 2017).

### Selection of Potential SB239063-resistant Virus Variants

Vero cells were infected with BPXV at MOI of 0.1 in medium containing 0.05% DMSO or 2 µg/mL SB239063. At 48–72 hpi, supernatant was collected from the virus infected cells (named passage 1 [P1]) and quantified by plaque assay. Sixty such sequential passages were carried out. The original virus stock (P0), P60-SB239063 and P60-control viruses were used to infect Vero cells at an MOI of 0.1 with either 10 µg/mL SB239063 or 0.05% DMSO. At 48 hpi, viral titers in the infected cell culture supernatant were quantified by plaque assay.

### Determination of Egg Lethal Dose 50 (LD<sub>50</sub>)

Specific pathogen free (SPF) embryonated chicken eggs were procured from Indovax Pvt. Ltd. Hisar, India. LD<sub>50</sub> of CGP57380 was determined by inoculating 5-fold serial dilutions of SB239063 (concentration ranging from 50 to 0.002 µg/egg) or equivalent volumes of DMSO, in 10 days old embryonated SPF eggs, in a total of 100 µL volumes CAM route. Eggs were examined for the viability of the embryos by candling for up to five days post-inoculation to determine the LD<sub>50</sub> by the Reed-Muench method.

### In vivo Antiviral Efficacy (EC<sub>50</sub>)

SPF embryonated chicken eggs, in triplicates, were inoculated with five-fold serial dilutions (25 to 0.1 µg/egg) of SB239063 or equal volumes of DMSO via the CAM route, followed by infection with BPXV at 100EID<sub>50</sub>. At 5–7 dpi, eggs were examined for pock lesions and/or death of the

embryos. EC<sub>50</sub> was determined by the Reed-Muench method.

### Generation of Plasmid Constructs Expressing sgRNA/Cas9 Complex

The mRNA sequences of p38- $\alpha$  (MAPK14) (GenBank Accession Number: XM\_007972807.1 to XM\_007972815.1, eight transcript variants), and p38- $\gamma$  (MAPK12) (GenBank Accession Number: XM\_007976194.1 to XM\_007976202.1, nine transcript variants) from African green monkey (*Chlorocebus sabaeus*) were retrieved from the GenBank and aligned using Clustal Omega to identify conserved regions among different transcript variants. For each target gene, at least four sgRNAs were designed by using an online program (<https://portals.broadinstitute.org/gpp/public/analysis-tools/gRNA-design>). Twenty nucleotide long sgRNAs-encoding sequences (supplementary table S2, Supplementary Material online) were cloned into pL.CRISPR.EFS.GFP at *BsmBI* site.

### Transfection

Vero cells were simultaneously transfected with 3 µg of each of the four plasmids in a 25 cm<sup>2</sup> cell culture flask using Lipofectamine 3000 (Thermo Fisher Scientific, Waltham, MA, USA).

### Sorting (FACS)

At 48 h following transfection, GFP expressing cells were sorted by FACS at Translational and Health Science Technology Institute (THSTI), Faridabad, India. The sorted cells were cultured in 96 well cell culture plates by limiting dilution assay. Wells with a single clone were selected for further propagation (scale up). Eleven clones from each of p38- $\alpha$  KO and p38- $\gamma$  KO cells were selected. After achieving sufficient number (usually a confluent 25 cm<sup>2</sup> flask), cells were analyzed for editing of the targeted gene.

### Validation of Gene Editing

For initial confirmation, out of the 11 clones each of the p38- $\alpha$  KO and p38- $\gamma$  KO propagated, 3 clones of p38- $\alpha$  and 4 clones of p38- $\gamma$  were subjected to total RNA extraction, cDNA synthesis and amplification of the target gene by PCR. Primers used to amplify the flanking regions in the target gene are depicted in supplementary table S3, Supplementary Material online. To further confirm, selected clones were also subjected to nucleotide sequencing. Finally, the clones were evaluated for disruption of the target gene by expression of the target protein (p38- $\alpha$  or p38- $\gamma$ ) in Western blot analysis.

### CHIP Assay

CHIP assay was carried out to evaluate the interaction of viral mRNA with eIF4E as per the previously described method (Kumar et al. 2021). Briefly, Vero cells, in triplicates, were infected with BPXV at MOI of 5. At 10 hpi, the cells were treated with 1% formaldehyde for 10 min

to covalently cross-link interacting proteins and nucleic acid. Thereafter, the cross-linking reaction was stopped by addition of 125 mM glycine (final concentration) and the cells were washed with ice-cold PBS. The cell lysates were prepared in immunoprecipitation (IP) buffer (150 mM NaCl, 50 mM Tris-HCl [pH 7.5], 5 mM EDTA, 0.5% NP-40, 1% Triton X-100 plus protease and phosphatase inhibitor cocktail) and sonicated in a Qsonica Sonicator Q500 (Qsonica, Newtown, CT, USA) (6 pulse of 15 sec at amplitude of 40%). The cell lysates were then centrifuged for 10 min at 12,000 g. The clarified cell lysates were mixed with 10 units of RiboLock RNase Inhibitor (Thermo Scientific, USA) and then incubated with the  $\alpha$ -pelf4E (reactive antibody),  $\alpha$ -pERK (nonreactive antibody) or equivalent volume of IP buffer (beads control) for 45 min at room temperature. Thereafter, 40  $\mu$ L (5 ng/ $\mu$ L) of Protein A Sepharose<sup>®</sup> slurry, prepared as per the instructions of the manufacturer (Abcam, USA) was added into each reaction and incubated overnight at 4 °C on a rotary platform. The beads were then washed 5 times in IP buffer (without protease inhibitors). To reverse the cross-linking, the complexes were then incubated with Proteinase K (20 mg/mL final concentration) at 56 °C for 40 minutes. Finally, the reaction mixtures were centrifuged at 12,000 g for 1 min and the supernatant was subjected to RNA isolation. The RNA was converted into cDNA and thereafter the levels of BPXV M gene was quantified by qRT-PCR.

### Whole Genome Sequencing of BPXV-P60-SB239063 and BPXV-P60-Control Viruses

BPXV-P60-SB239063 and BPXV-P60-Control grow at a titer of  $\sim 10^7$  PFU/mL. BPXV. These viruses were further concentrated (10-times) by ultracentrifugation and subjected to DNA isolation by DNeasy Blood & Tissue Kit (Qiagen, USA). Libraries were prepared using Illumina<sup>®</sup> DNA Prep, (M) Tagmentation kit (Illumina Inc., USA) and checked on Bionalyzer 2100 (Agilent, CA, USA) using DNA High Sensitivity Assay kit (Agilent, CA, USA). For library quantification, we used Qubit Fluorometer v4.0 and Qubit 1x dsDNA assay kit (Thermo Fisher Scientific, MA, USA). Sequencing was performed on Illumina MiSeq system using MiSeq reagents kit V2 500 cycles (2  $\times$  250) paired-end chemistry. Low quality data were trimmed and filtered using PRINSEQ (Schmieder and Edwards 2011) with the following parameters; dynamic trimming to remove bad quality ends with an average quality of 25 within 10 bp sliding window and reads with minimum length of 150 bases were discarded. Data were then imported into the CLC Genomics Workbench Version 22.0.1 with the in-house pipeline (supplementary fig. S4, Supplementary Material online) where we used realignment algorithm of CLC genomics workbench to correct read mappings over INDELS with guided track with initial variant calling tracks. Reference based consensus were called using the variant table generated to extract the genome sequence of the respective samples. To visualize and

compare each variant called by the CLC genomics workbench we used IGV version 2.4.14.

### Supplementary Material

Supplementary data are available at *Molecular Biology and Evolution* online.

### Acknowledgments

This work was supported by the Science and Engineering Research Board, Department of Science and Technology, Government of India (grant number CVD/2020/000103, CRG/2018/004747 and CRG/2019/000829 to N. Kumar and S. Barua). A part of this study belongs to the PhD thesis work of Yogesh Chander.

### Data Availability

Vero cell adapted BPXV was deposited in the National Centre for Veterinary Type Cultures (NCVTC), Hisar with an Accession Number of VTCC-AVA90 which can be accessed at <http://ncvtc.org.in/wp-content/uploads/2019/08/Viruses-available-for-distribution.pdf>. Its whole genome sequence is available in GenBank with an Accession Number of MW883892.1. The whole genome sequences of BPXV-P60-SB239063 and BPXV-P60-Control were deposited to GenBank under the Accession Numbers of ON974728 and ON974727 respectively. All the other data needed to evaluate the conclusion in this article are available in the Supplementary Material.

### References

- Adamson AL, Darr D, Holley-Guthrie E, Johnson RA, Mauser A, Swenson J, Kenney S. 2000. Epstein-Barr virus immediate-early proteins BZLF1 and BRLF1 activate the ATF2 transcription factor by increasing the levels of phosphorylated p38 and c-Jun N-terminal kinases. *J Virol.* **74**:1224–1233.
- Avitzour M, Diskin R, Raboy B, Askari N, Engelberg D, Livnah O. 2007. Intrinsically active variants of all human p38 isoforms. *FEBS J.* **274**: 963–975.
- Banerjee S, Narayanan K, Mizutani T, Makino S. 2002. Murine coronavirus replication-induced p38 mitogen-activated protein kinase activation promotes interleukin-6 production and virus replication in cultured cells. *J Virol.* **76**:5937–5948.
- Bauer L, Lyoo H, van der Schaar HM, Strating JR, van Kuppeveld FJ. 2017. Direct-acting antivirals and host-targeting strategies to combat enterovirus infections. *Curr Opin Virol.* **24**:1–8.
- Baxby D. 1969. Variability in the characteristics of pocks produced on the chick chorioallantois by white pock mutants of cowpox and other poxviruses. *J Hyg (Lond).* **67**:637–647.
- Chander Y, Kumar R, Khandelwal N, Singh N, Shringi BN, Barua S, Kumar N. 2021. Role of p38 mitogen-activated protein kinase signalling in virus replication and potential for developing broad spectrum antiviral drugs. *Rev Med Virol.* **31**:1–16.
- Chaudhary K, Chaubey KK, Singh SV, Kumar N. 2015. Receptor tyrosine kinase signaling regulates replication of the peste des petits ruminants virus. *Acta Virol.* **59**:78–83.
- Chen Y, Wang L, Jin J, Luan Y, Chen C, Li Y, Chu H, Wang X, Liao G, Yu Y. 2017. P38 inhibition provides anti-DNA virus immunity by

- regulation of USP21 phosphorylation and STING activation. *J Exp Med.* **214**:991–1010.
- Cheng Y, Sun F, Wang L, Gao M, Xie Y, Sun Y, Liu H, Yuan Y, Yi W, Huang Z. 2020. Virus-induced p38 MAPK activation facilitates viral infection. *Theranostics* **10**:12223.
- Choi M-S, Heo J, Yi C-M, Ban J, Lee N-J, Kim SW, Kim N-J, Inn K-S. 2016. A novel p38 mitogen activated protein kinase (MAPK) specific inhibitor suppresses respiratory syncytial virus and influenza A virus replication by inhibiting virus-induced p38 MAPK activation. *Biochem Biophys Res Commun.* **477**:311–316.
- Cook M. 2016. The role of MAPK p38 stress pathway-induced cellular translation in human and macaque cells targeted during B virus infection [dissertation]. Georgia State University. doi:10.57709/8474771
- Cuadrado A, Nebreda AR. 2010. Mechanisms and functions of p38 MAPK signalling. *Biochem J.* **429**:403–417.
- Cuenda A, Cohen P, Buee-Scherrer V, Goedert M. 1997. Activation of stress-activated protein kinase-3 (SAPK3) by cytokines and cellular stresses is mediated via SAPKK3 (MKK6); comparison of the specificities of SAPK3 and SAPK2 (RK/p38). *EMBO J.* **16**:295–305.
- Cuenda A, Rousseau S. 2007. p38 MAP-kinases pathway regulation, function and role in human diseases. *Biochim Biophys Acta* **1773**:1358–1375.
- Datta P, Ukey R, Bruiners N, Honnen W, Carayannopoulos MO, Reichman C, Choudhary A, Onyuka A, Handler D, Guerrini V, Mishra PK, Dewald HK, Lardizabal A, Lederer L, Leiser AL, Hussain S, Jagpal SK, Radbel J, Bhowmick T, Horton DB, Barrett ES, Xie YL, Fitzgerald-Bocarsly P, Weiss SH, Woortman M, Parmar H, Roy J, Dominguez-Bello MG, Blaser MJ, Carson JL, Panettieri RA, Jr., Libutti SK, Raymond HF, Pinter A, Gennaro ML. 2021. Highly versatile antibody binding assay for the detection of SARS-CoV-2 infection. *medRxiv*. doi:10.1101/2021.07.09.21260266
- Dou D, Revol R, Östbye H, Wang H, Daniels R. 2018. Influenza A virus cell entry, replication, virion assembly and movement. *Front Immunol.* **9**:1581.
- Enslin H, Raingeaud J, Davis RJ. 1998. Selective activation of p38 mitogen-activated protein (MAP) kinase isoforms by the MAP kinase kinases MKK3 and MKK6. *J Biol Chem.* **273**:1741–1748.
- Halfmann P, Neumann G, Kawaoka Y. 2011. The Ebola virus VP24 protein blocks phosphorylation of p38 mitogen-activated protein kinase. *J Infect Dis.* **204**(Suppl 3):S953–S956.
- Han J, Wu J, Silke J. 2020. An overview of mammalian p38 mitogen-activated protein kinases, central regulators of cell stress and receptor signaling. *F1000Res.* **9**:1–20.
- Higgins CA, Nilsson-Payant BE, Kurland A, Adhikary P, Golyner I, Danziger O, Panis M, Rosenberg BR, Johnson JR. 2021. SARS-CoV-2 hijacks p38 $\beta$ /MAPK11 to promote viral protein translation. *bioRxiv*. doi:10.1101/2021.08.20.457146
- Hoffmann HH, Kunz A, Simon VA, Palese P, Shaw ML. 2011. Broad-spectrum antiviral that interferes with de novo pyrimidine biosynthesis. *Proc Natl Acad Sci U S A.* **108**:5777–5782.
- Hopcraft SE, Evans MJ. 2015. Selection of a hepatitis C virus with altered entry factor requirements reveals a genetic interaction between the E1 glycoprotein and claudins. *Hepatology* **62**:1059–1069.
- Jiang Y, Chen C, Li Z, Guo W, Gegner JA, Lin S, Han J. 1996. Characterization of the structure and function of a new mitogen-activated protein kinase (p38beta). *J Biol Chem.* **271**:17920–17926.
- Jiang Y, Gram H, Zhao M, New L, Gu J, Feng L, Di Padova F, Ulevitch RJ, Han J. 1997. Characterization of the structure and function of the fourth member of p38 group mitogen-activated protein kinases, p38delta. *J Biol Chem.* **272**:30122–30128.
- Khandelwal N, Chander Y, Kumar R, Riyesh T, Dedar RK, Kumar M, Gulati BR, Sharma S, Tripathi BN, Barua S, et al. 2020. Antiviral activity of Apigenin against buffalopox: novel mechanistic insights and drug-resistance considerations. *Antiviral Res.* **181**:104870.
- Khandelwal N, Chander Y, Rawat KD, Riyesh T, Nishanth C, Sharma S, Jindal N, Tripathi BN, Barua S, Kumar N. 2017. Emetine inhibits replication of RNA and DNA viruses without generating drug-resistant virus variants. *Antiviral Res.* **144**:196–204.
- Krumm SA, Ndungu JM, Yoon JJ, Dochow M, Sun A, Natchus M, Snyder JP, Plemper RK. 2011. Potent host-directed small-molecule inhibitors of myxovirus RNA-dependent RNA-polymerases. *PLoS One* **6**:e20069.
- Kuma Y, Sabio G, Bain J, Shpiro N, Marquez R, Cuenda A. 2005. BIRB796 inhibits all p38 MAPK isoforms in vitro and in vivo. *J Biol Chem.* **280**:19472–19479.
- Kumar R, Afsar M, Khandelwal N, Chander Y, Riyesh T, Dedar RK, Gulati BR, Pal Y, Barua S, Tripathi BN, et al. 2021. Emetine suppresses SARS-CoV-2 replication by inhibiting interaction of viral mRNA with eIF4E. *Antiviral Res.* **189**:105056.
- Kumar R, Khandelwal N, Chander Y, Nagori H, Verma A, Barua A, Godara B, Pal Y, Gulati BR, Tripathi BN, et al. 2022. S-adenosylmethionine-dependent methyltransferase inhibitor DZNep blocks transcription and translation of SARS-CoV-2 genome with a low tendency to select for drug-resistant viral variants. *Antiviral Res.* **197**:105232.
- Kumar R, Khandelwal N, Chander Y, Riyesh T, Tripathi BN, Kashyap SK, Barua S, Maherchandani S, Kumar N. 2018a. MNK1 inhibitor as an antiviral agent suppresses buffalopox virus protein synthesis. *Antiviral Res.* **160**:126–136.
- Kumar N, Khandelwal N, Kumar R, Chander Y, Rawat KD, Chaubey KK, Sharma S, Singh SV, Riyesh T, Tripathi BN, et al. 2019. Inhibitor of sarco/endoplasmic reticulum calcium-ATPase impairs multiple steps of paramyxovirus replication. *Front Microbiol.* **10**:209.
- Kumar R, Khandelwal N, Thachamvally R, Tripathi BN, Barua S, Kashyap SK, Maherchandani S, Kumar N. 2018b. Role of MAPK/MNK1 signaling in virus replication. *Virus Res.* **253**:48–61.
- Kumar N, Liang Y, Parslow TG, Liang Y. 2011a. Receptor tyrosine kinase inhibitors block multiple steps of influenza A virus replication. *J Virol.* **85**:2818–2827.
- Kumar N, Maherchandani S, Kashyap SK, Singh SV, Sharma S, Chaubey KK, Ly H. 2014. Peste des petits ruminants virus infection of small ruminants: a comprehensive review. *Viruses* **6**:2287–2327.
- Kumar S, McDonnell PC, Gum RJ, Hand AT, Lee JC, Young PR. 1997. Novel homologues of CSBP/p38 MAP kinase: activation, substrate specificity and sensitivity to inhibition by pyridinyl imidazoles. *Biochem Biophys Res Commun.* **235**:533–538.
- Kumar N, Sharma S, Kumar R, Tripathi BN, Barua S, Ly H, Rouse BT. 2020. Host-Directed antiviral therapy. *Clin Microbiol Rev.* **33**:e00168-19.
- Kumar N, Sharma NR, Ly H, Parslow TG, Liang Y. 2011b. Receptor tyrosine kinase inhibitors that block replication of influenza A and other viruses. *Antimicrob Agents Chemother.* **55**:5553–5559.
- Kumar N, Xin ZT, Liang Y, Ly H, Liang Y. 2008. NF-kappaB signaling differentially regulates influenza virus RNA synthesis. *J Virol.* **82**:9880–9889.
- Lamarque MJ, Borawski J, Bose A, Capacci-Daniel C, Colvin R, Dennehy M, Ding J, Dobler M, Drumm J, Gaither LA, et al. 2012. Anti-hepatitis C virus activity and toxicity of type III phosphatidylinositol-4-kinase beta inhibitors. *Antimicrob Agents Chemother.* **56**:5149–5156.
- Livak KJ, Schmittgen TD. 2001. Analysis of relative gene expression data using real-time quantitative PCR and the 2(-Delta Delta C(T)) method. *Methods* **25**:402–408.
- Long JS, Mistry B, Haslam SM, Barclay WS. 2019. Host and viral determinants of influenza A virus species specificity. *Nat Rev Microbiol.* **17**:67–81.
- Lv L, Zhang L. 2021. Host proviral and antiviral factors for SARS-CoV-2. *Virus Genes* **57**:475–488.
- Marchant D, Dou Y, Luo H, Garmaroudi FS, McDonough JE, Si X, Walker E, Luo Z, Arner A, Hegele RG. 2009. Bosentan enhances viral load via endothelin-1 receptor type-A-mediated p38 mitogen-activated protein kinase activation while improving cardiac function during coxsackievirus-induced myocarditis. *Circ Res.* **104**:813–821.



- Marennikova SS, Shelukhina EM, Shenkman LS. 1973. Role of the temperature of incubation of infected chick embryos in the differentiation of certain poxviruses according to pock morphology. *Acta Virol.* **17**:362.
- Marinaik CB, Venkatesha MD, Gomes AR, Reddy P, Nandini P, Byregowda SM. 2018. Isolation and molecular characterization of zoonotic Buffalopox virus from skin lesions of humans in India. *Int J Dermatol.* **57**:590–592.
- Mihail SM, Wangzhou A, Kunjilwar KK, Moy JK, Dussor G, Walters ET, Price TJ. 2019. MNK-eIF4E signalling is a highly conserved mechanism for sensory neuron axonal plasticity: evidence from *Aplysia californica*. *Philos Trans R Soc Lond B Biol Sci.* **374**:20190289.
- Mikkelsen SS, Jensen SB, Chiliveru S, Melchjorsen J, Julkunen I, Gaestel M, Arthur JSC, Flavell RA, Ghosh S, Paludan SR. 2009. RIG-I-mediated activation of p38 MAPK is essential for viral induction of interferon and activation of dendritic cells. *J Biol Chem.* **284**:10774–10782.
- Mudaliar P, Pradeep P, Abraham R, Sreekumar E. 2021. Targeting cap-dependent translation to inhibit chikungunya virus replication: selectivity of p38 MAPK inhibitors to virus-infected cells due to autophagy-mediated down regulation of phospho-ERK. *J Gen Virol.* **102**:001629.
- Nagaleekar VK, Sabio G, Aktan I, Chant A, Howe IW, Thornton TM, Benoit PJ, Davis RJ, Rincon M, Boyson JE. 2011. Translational control of NKT cell cytokine production by p38 MAPK. *J Immunol.* **186**:4140–4146.
- Nayak TK, Mamidi P, Sahoo SS, Kumar PS, Mahish C, Chatterjee S, Subudhi BB, Chattopadhyay S, Chattopadhyay S. 2019. P38 and JNK mitogen-activated protein kinases interact with chikungunya virus non-structural protein-2 and regulate TNF induction during viral infection in macrophages. *Front Immunol.* **10**:786.
- Pashenkov MV, Balyasova LS, Dagil YA, Pinegin BV. 2017. The role of the p38-MNK-eIF4E signaling axis in TNF production downstream of the NOD1 receptor. *J Immunol.* **198**:1638–1648.
- Pawlotsky JM. 2012. The science of direct-acting antiviral and host-targeted agent therapy. *Antivir Ther.* **17**:1109–1117.
- Peng H, Shi M, Zhang L, Li Y, Sun J, Zhang L, Wang X, Xu X, Zhang X, Mao Y. 2014. Activation of JNK1/2 and p38 MAPK signaling pathways promotes enterovirus 71 infection in immature dendritic cells. *BMC Microbiol.* **14**:1–9.
- Penrose KJ, Garcia-Alai M, de Prat-Gay G, McBride AA. 2004. Casein kinase II phosphorylation-induced conformational switch triggers degradation of the papillomavirus E2 protein. *J Biol Chem.* **279**:22430–22439.
- Ratcliff AN, Shi W, Arts EJ. 2013. HIV-1 resistance to maraviroc conferred by a CD4 binding site mutation in the envelope glycoprotein gp120. *J Virol.* **87**:923–934.
- Risco A, Cuenda A. 2012. New insights into the p38gamma and p38delta MAPK pathways. *J Signal Transduct.* **2012**:520289.
- Rodriguez Limardo RG, Ferreira DN, Roitberg AE, Marti MA, Turjanski AG. 2011. P38gamma activation triggers dynamical changes in allosteric docking sites. *Biochemistry* **50**:1384–1395.
- Roy P, Chandramohan A. 2021. Buffalopox disease in livestock and milkers, India. *Emerg Infect Dis.* **27**:1989–1991.
- Schmieder R, Edwards R. 2011. Quality control and preprocessing of metagenomic datasets. *Bioinformatics* **27**: 863–864.
- Schuck S, Ruse C, Stenlund A. 2013. CK2 Phosphorylation inactivates DNA binding by the papillomavirus E1 and E2 proteins. *J Virol.* **87**:7668–7679.
- Shveygert M, Kaiser C, Bradrick SS, Gromeier M. 2010. Regulation of eukaryotic initiation factor 4E (eIF4E) phosphorylation by mitogen-activated protein kinase occurs through modulation of Mnk1-eIF4G interaction. *Mol Cell Biol.* **30**:5160–5167.
- Singh RK, Hosamani M, Balamurugan V, Bhanuprakash V, Rasool TJ, Yadav MP. 2007. Buffalopox: an emerging and re-emerging zoonosis. *Anim Health Res Rev.* **8**:105–114.
- Skaug B, Chen ZJ. 2010. Emerging role of ISG15 in antiviral immunity. *Cell* **143**:187–190.
- Stramucci L, Pranteda A, Bossi G. 2018. Insights of crosstalk between p53 protein and the MKK3/MKK6/p38 MAPK signaling pathway in cancer. *Cancers (Basel)* **10**:131.
- Su A-r, Qiu M, Li Y-l, Xu W-t, Song S-w, Wang X-h, Song H-y, Zheng N, Wu Z-w. 2017. BX-795 inhibits HSV-1 and HSV-2 replication by blocking the JNK/p38 pathways without interfering with PDK1 activity in host cells. *Acta Pharmacol Sin.* **38**:402–414.
- Sugasti-Salazar M, Llamas-González YY, Campos D, González-Santamaría J. 2021. Inhibition of p38 mitogen-activated protein kinase impairs mayaro virus replication in human dermal fibroblasts and HeLa cells. *Viruses* **13**:1156.
- van der Linden L, Wolthers KC, van Kuppeveld FJ. 2015. Replication and inhibitors of enteroviruses and parechoviruses. *Viruses* **7**: 4529–4562.
- Wei L, Zhu S, Wang J, Zhang C, Quan R, Yan X, Liu J. 2013. Regulatory role of ASK1 in porcine circovirus type 2-induced apoptosis. *Virology* **447**:285–291.
- Xu X, Miao J, Shao Q, Gao Y, Hong L. 2020. Apigenin suppresses influenza A virus-induced RIG-I activation and viral replication. *J Med Virol.* **92**:3057–3066.
- Yadav PD, Mauldin MR, Nyayanit DA, Albarino CG, Sarkale P, Shete A, Guerrero LW, Nakazawa Y, Nichol ST, Mourya DT. 2020. Isolation and phylogenomic analysis of buffalopox virus from human and buffaloes in India. *Virus Res.* **277**:197836.
- Yang Z, Zhang X, Darrah PA, Mosser DM. 2010. The regulation of Th1 responses by the p38 MAPK. *J Immunol.* **185**:6205–6213.
- Zachos G, Clements B, Conner J. 1999. Herpes simplex virus type 1 infection stimulates p38/c-Jun N-terminal mitogen-activated protein kinase pathways and activates transcription factor AP-1. *J Biol Chem.* **274**:5097–5103.
- Zhan Y, Yu S, Yang S, Qiu X, Meng C, Tan L, Song C, Liao Y, Liu W, Sun Y. 2020. Newcastle Disease virus infection activates PI3K/Akt/mTOR and p38 MAPK/Mnk1 pathways to benefit viral mRNA translation via interaction of the viral NP protein and host eIF4E. *PLoS Pathog.* **16**:e1008610.